npg

Smac mimetic promotes glioblastoma cancer stem-like cell differentiation by activating NF-κB

A Tchoghandjian[1], C Jennewein[1], I Eckhardt[1], S Momma[2], D Figarella-Branger[3] and S Fulda*,[1]

Recently, a broader role of inhibitor of apoptosis (IAP) proteins besides their antiapoptotic functions has been described. Therefore, we investigated the effect of non-toxic concentrations of the small-molecule Smac mimetic BV6, which antagonizes IAP proteins, on differentiation of cancer stem-like cells (CSLCs) derived from primary glioblastoma (GBM) specimens. Here, we identify a novel function of BV6 in regulating differentiation of GBM CSLCs by activating NF-κB. BV6 at non-lethal doses stimulates morphological changes associated with the differentiation of GBM CSLCs. BV6 increases transcriptional activity, mRNA and protein levels of the astrocytic marker GFAP without altering expression of the neuronal marker β-III-tubulin, indicating that BV6 induces astrocytic differentiation of GBM CSLCs. Molecular studies reveal that BV6 triggers processing of the NF-κB subunit p100 to p52, nuclear translocation of p52 and p50 and increased NF-κB DNA-binding. Intriguingly, inhibition of NF-κB by overexpression of dominant-negative IκBα super-repressor (IκBα-SR) blocks the BV6-stimulated increase in GFAP and differentiation. Interestingly, this BV6-stimulated differentiation is associated with reduced expression of stemness markers such as CD133, Nanog and Sox2 in GBM CSLCs. In contrast, BV6 does not alter cell morphology, differentiation and expression of stemness markers in non-malignant neural stem cells. Importantly, BV6 treatment reduces clonogenicity of GBM CSLCs *in vitro* and *in vivo*, suppresses their tumorigenicity in orthotopic and subcutaneous mouse models and significantly increases the survival of mice. By identifying a novel role of BV6 in promoting differentiation of GBM CSLCs, these findings provide new insights into Smac mimetic-regulated non-apoptotic functions with important implications for targeting GBM CSLCs.

Cell Death and Differentiation (2014) 21, 735–747; doi:10.1038/cdd.2013.200; published online 31 January 2014

Glioblastoma multiforme (GBM) is the most common and aggressive primary brain tumor in adults.[1] The median survival is very low and no curative treatment is currently available,[2] thus calling for novel treatment approaches. GBM is heterogeneous and composed of vascular, inflammatory and stromal cells in addition to neoplastic cells.[3] Within the neoplastic compartment, a subpopulation of cells was described as CSLCs.[4,5] As CSLCs have been implicated in resistance to chemo- and radiotherapy[6] and have recently been shown to sustain long-term tumor growth *in vivo* after chemotherapy and to cause tumor recurrence,[7] they are considered as critical therapeutic targets in GBM. One approach to tackle CSLCs resides in the induction of differentiation to suppress their stem cell properties and tumorigenic potential. Indeed, previous studies have highlighted the potential of therapeutic strategies to trigger differentiation of GBM CSLCs, for example using interferon-β (IFN-β),[8] all-trans retinoic acid,[9] bone morphogenic proteins[10] or microRNAs.[11,12]

Inhibitors of apoptosis (IAP) proteins are often over-expressed in human cancers including GBM and their expression levels correlate with poor prognosis and treatment resistance.[13,14] While some IAP proteins such as X-linked inhibitor of apoptosis protein (XIAP) are well characterized for their antiapoptotic properties, they are now recognized to have a broader role in tumor biology as they also regulate additional signal transduction pathways such as nuclear factor κB (NF-κB) signaling.[15] There are two NF-κB signaling pathways, that is, the canonical (classical) and the non-canonical (alternative) pathway.[16] The canonical NF-κB pathway is, for example, initiated upon binding of tumor necrosis factor (TNF)α to tumor necrosis factor (TNF) receptor (TNFR)1, which leads to the activation of the IKK complex, phosphorylation and degradation of IκBα, translocation of p65/p50 dimers into the nucleus and transcriptional activation of NF-κB target genes. The non-canonical NF-κB signaling pathway is engaged by, for example, CD40 ligand or tumor necrosis factor-like weak inducer of apoptosis (TWEAK) via

accumulation of NF-κB-inducing kinase (NIK), which phosphorylates IKKα leading to processing of p100 to p52. As a result, p52 and RelB translocate into the nucleus to activate NF-κB target gene expression. The E3 ligase activity of cellular inhibitor of apoptosis (cIAP) proteins on one side promotes canonical NF-κB pathway activation by adding K63-linked ubiquitin chains on the serine/threonine kinase receptor-interacting protein (RIP)1, and on the other side blocks non-canonical NF-κB activation by ubiquitinylation and proteasomal degradation of NIK.[17–20]

Small-molecule IAP inhibitors such as Smac mimetics that mimic the N-terminal part of Smac were developed to antagonize IAP proteins and were reported to either directly trigger cell death or to sensitize cancer cells to various cytotoxic therapies.[15] Previously, we reported that IAP inhibitors increase the radiosensitivity of GBM cells including GBM CSLCs by lowering the threshold for apoptosis induction.[21,22] However, the question whether or not IAP inhibitors also regulate additional cellular functions beyond apoptosis in GBM CSLCs has not yet been addressed. Therefore, in this study we investigated the role of the Smac mimetic BV6[23] in the regulation of differentiation of GBM CSLCs.

Results

Smac mimetic stimulates differentiation of GBM CSLCs. As IAP proteins have been described to exert non-apoptotic functions,[24,25] we investigated whether the Smac mimetic BV6 regulates differentiation of GBM CSLCs at non-toxic concentrations that engage signaling pathways without triggering cell death. To this end, we initially determined non-lethal doses of BV6 in two GBM CSLCs (GBM9 and GBM10) derived from primary tumor specimens.[26] Analysis of the p53 and PTEN status indicates that GBM9 cells are p53 wild-type and express PTEN protein although at somewhat reduced levels, while GBM10 cells are p53 mutant and lack wild-type PTEN protein expression (Supplementary Figure S1A). To explore cancer cell-specific effects of BV6, we also used non-malignant neural stem cells (NSCs) that we recently characterized.[27] Up to a concentration of 1 μM, BV6 did not reduce cell viability or induce caspase-3 activation in GBM CSLCs or NSCs (Figures 1a and b). In parallel, we monitored the effect of BV6 on expression levels of IAP proteins. BV6 profoundly reduced cIAP1 expression in all three cell lines (Figure 1b). In addition, BV6 caused downregulation of XIAP in GBM9 and GBM10 cells and to a minor extent in NSCs and also slightly decreased cIAP2 expression in GBM10 cells, while cIAP2 was very weakly expressed in GBM9 cells and NSCs (Figure 1b). For subsequent experiments, we therefore used 0.6–1 μM BV6 as non-toxic concentrations that affect cellular signaling pathways as indicated by cIAP1 degradation.

As cellular differentiation is associated with typical morphological changes, we analyzed the morphology of GBM9, GBM10 and NSCs cells after treatment with BV6. Interestingly, exposure to BV6 triggered a significant increase in the cell elongation of GBM9 and GBM10 cells, whereas it caused no phenotypic changes in NSCs (Figures 1c and d). This indicates that BV6 at sublethal concentrations triggers

morphological changes associated with cellular differentiation in GBM CSLCs but not in non-malignant NSCs.

Smac mimetic increases astrocytic differentiation marker GFAP in GBM CSLCs. We next investigated whether BV6 regulates expression levels of neural differentiation markers. To this end, we focused on the two major neural lineages by analyzing astrocytic differentiation using GFAP expression and neuronal differentiation using β-III-tubulin expression. Interestingly, BV6 significantly increased the amount of GFAP-positive cells in GBM9 and GBM10 cells, whereas it did not alter GFAP expression in NSCs (Figures 2a–c). Control experiments showed that exposure to 2% fetal calf serum (FCS) stimulated GFAP expression in NSCs (Supplementary Figures S1B and C). By comparison, no changes in β-III-tubulin protein levels were found after BV6 treatment either in GBM CSLCs or in NSCs (Figures 2d–f), whereas stimulation with 2% FCS increased β-III-tubulin protein levels in NSCs (Supplementary Figures S1D and E).

As we found that BV6 treatment increases GFAP protein levels, we next asked whether this is due to transcriptional activation. To address this question, we analyzed GFAP mRNA levels and promoter activity. Of note, BV6 caused a significant increase in GFAP mRNA levels in both GBM9 and GBM10 cells (Figure 2g). In addition, BV6 significantly enhanced the transcriptional activity of the GFAP promoter as determined by luciferase assay (Figure 2h). To control that this BV6-stimulated GFAP expression is not simply due to changes in proliferation, we monitored in parallel cell numbers. BV6 treatment had no effect on cell numbers of GBM CSLCs or NSCs (Supplementary Figure S2), confirming that altered proliferation does not account for the BV6-stimulated increase in GFAP expression. Together, this set of experiments demonstrates that BV6 upregulates the astrocytic marker protein GFAP in GBM CSLCs but not in NSCs by increasing GFAP transcriptional activity as well as GFAP mRNA and protein levels, whereas BV6 does not alter expression of the neuronal marker β-III tubulin.

Smac mimetic activates NF-κB signaling in GBM CSLCs. As BV6 has been reported to stimulate NF-κB activation by depleting IAP proteins,[23] we then examined the effect of BV6 on NF-κB signaling in GBM CSLCs. BV6 stimulated increased NF-κB DNA-binding over a prolonged period of time up to at least 7 days (Figure 3a). Also, BV6 triggered processing of p100 to p52 in GBM CSLCs as well as in NSCs (Figure 3b, Supplementary Figure S3). To analyze which NF-κB subunits translocate into the nucleus, we prepared cytosolic and nuclear extracts. BV6 stimulated translocation of p52 and p50 into the nucleus, while no nuclear translocation of p65 was found (Figure 3c). TNFα was used as positive control for NF-κB activation (Figures 3a and c). Together, this set of experiments shows that BV6 activates NF-κB signaling in GBM CSLCs.

NF-κB is required for Smac mimetic-induced astrocytic differentiation of GBM CSLCs. We next asked whether NF-κB activation is required for BV6-induced astrocytic differentiation of GBM CSLCs. To address this question, we overexpressed IκBα-SR to inhibit NF-κB signaling
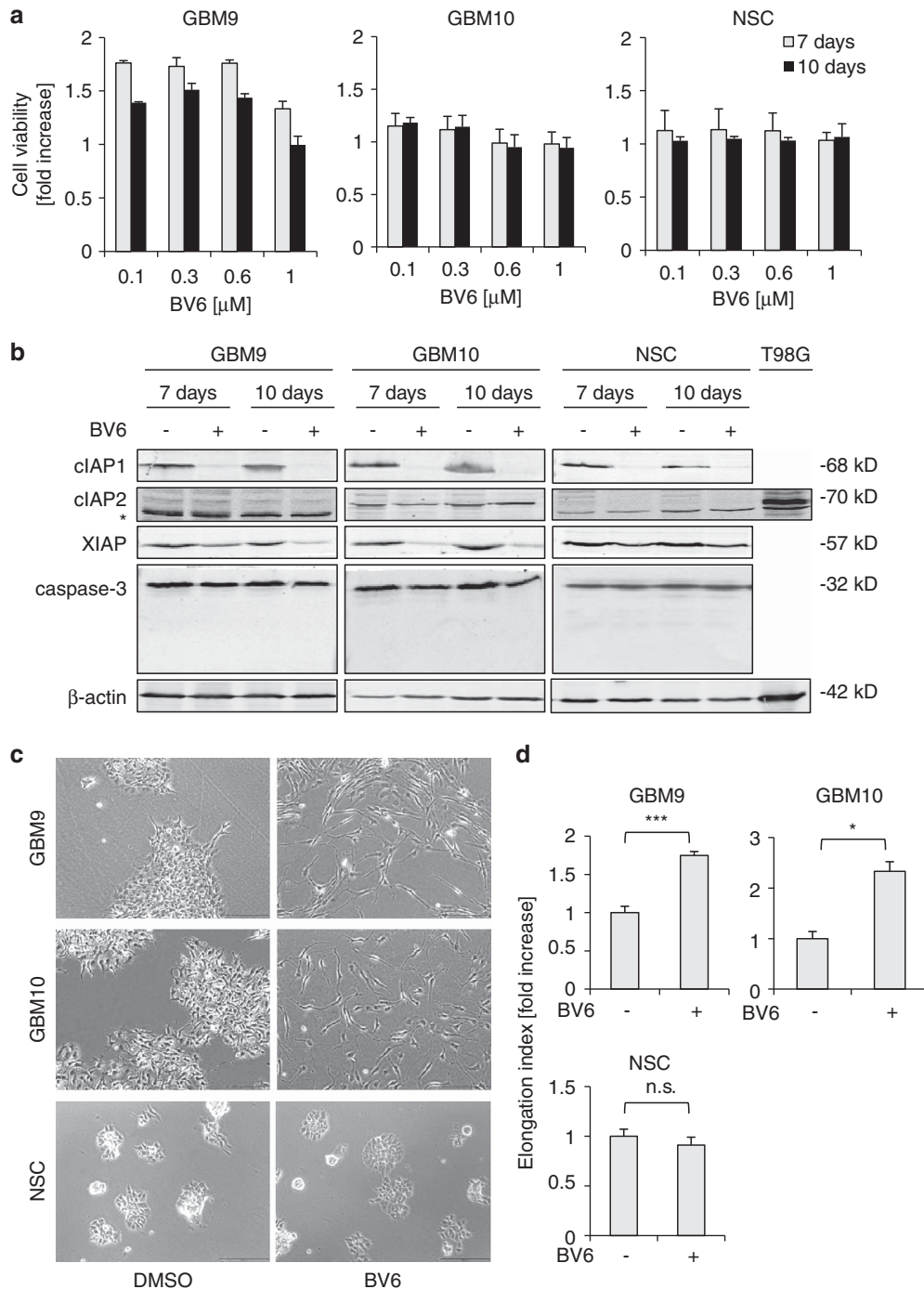
Figure 1 Smac mimetic triggers cell elongation of GBM CSLCs. (**a**) Cells were treated for 7 and 10 days with indicated concentrations of BV6 or DMSO. Cell viability was measured by MTT assay and is expressed as fold increase of untreated controls. (**b**) Cells were treated with 0.6 μM BV6 (GBM9) or 1 μM BV6 (GBM10, NSCs) for indicated times. Expression of cIAP1, cIAP2, XIAP and caspase-3 was analyzed by western blotting. T98G cells were used as a positive control for cIAP2 expression. Expression of β-actin served as loading control; *, unspecific band. (**c** and **d**) GBM9 cells were treated for 10 days with 0.6 μM BV6 or DMSO and GBM10 and NSCs for 7 days with 1 μM BV6 or DMSO. Cell morphology was analyzed by phase-contrast microscope; scale bar, 250 μm (**c**). Cell elongation was quantified by measuring cell length and width and by calculating cell elongation index (length/width); fold increase in cell elongation index in the presence and absence of BV6 is shown (**d**). In (**a** and **d**) mean + S.E.M. of three independent experiments performed in triplicate is shown; *P<0.05; ***P<0.001; n.s., not significant. Representative experiments of two (**b**) and three (**c**) independent experiments are shown

(Figure 4, Supplementary Figure S5A). Control experiments showed that inhibition of NF-κB by IκBα-SR did not significantly alter cell viability, apoptosis, cell cycle distribution or proliferation of GBM CSLCs upon treatment with BV6 (Supplementary Figures S4 and S5B). Also, NF-κB inhibition by IκBα-SR resulted in decreased constitutive expression of
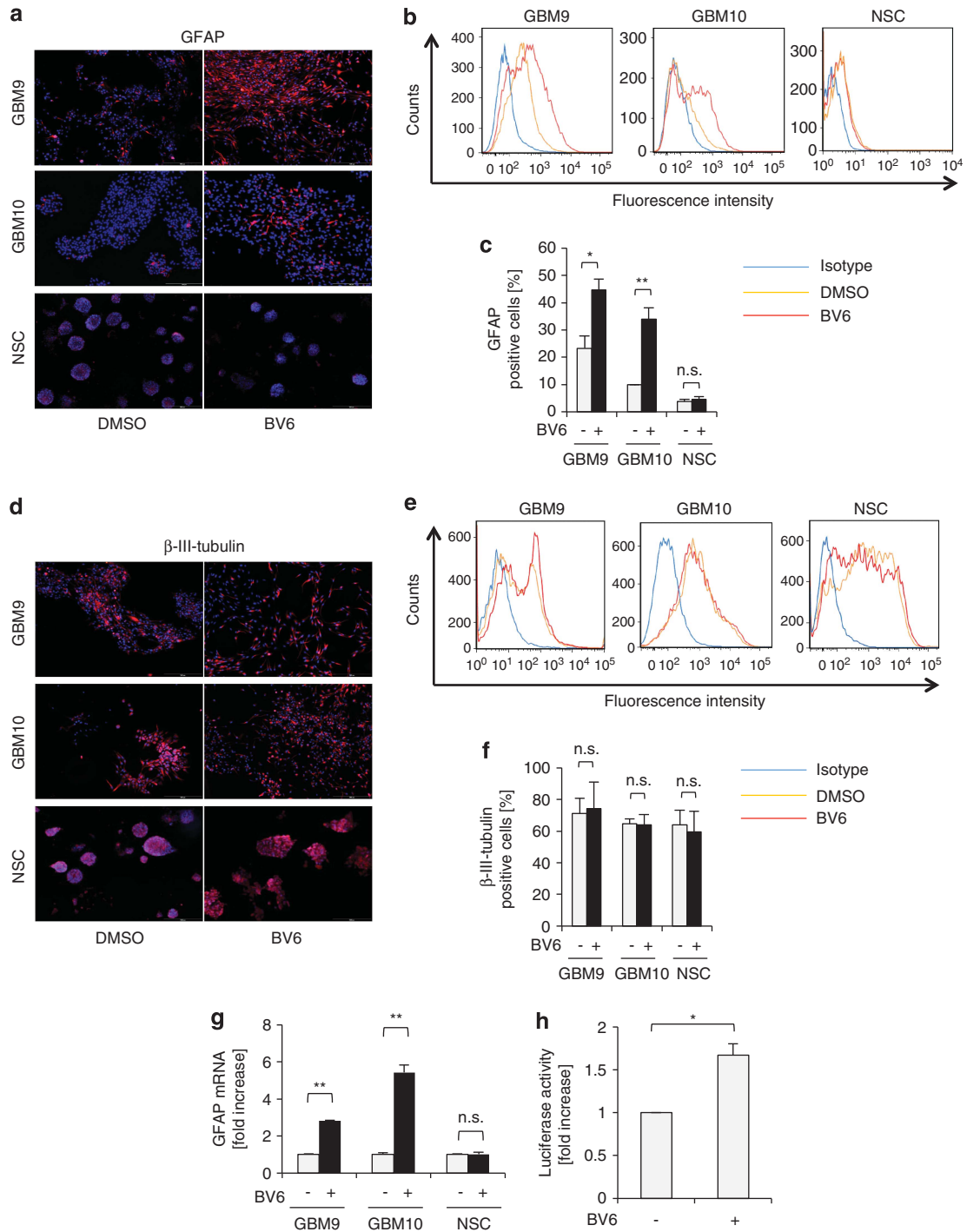
Figure 2 Smac mimetic triggers expression of GFAP astrocytic marker. (**a–g**) GBM9 cells were treated for 10 days with 0.6 μM BV6 or DMSO; GBM10 and NSCs for 7 days with 1 μM BV6 or DMSO. (**a**) Cells were fixed and stained with anti-GFAP antibody and counterstained with DAPI. Representative pictures of four independent experiments are shown. Scale bar, 500 μm. (**b** and **c**) Cells were dissociated and stained with anti-GFAP antibody and isotype control for FACS analysis (**b**). The percentage of GFAP-positive cells is shown (**c**). (**d**) Cells were fixed and stained with anti-β-III-tubulin antibody and counterstained with DAPI. Representative pictures of four independent experiments are shown. Scale bar, 500 μm. (**e** and **f**) Cells were dissociated and stained with anti-β-III-tubulin antibody and isotype control for FACS analysis (**d**). The percentage of β-III-tubulin-positive cells is presented (**e**). (**g**) GBM9 cells were treated for 10 days with 0.6 μM BV6 or DMSO and GBM10 and NSCs for 7 days with 1 μM BV6 or DMSO. GFAP mRNA levels were analyzed by quantitative RT-PCR and fold increase in GFAP mRNA levels is shown. Each experiment was performed in triplicate. (**h**) GBM10 cells were treated with 1 μM BV6 or DMSO. GFAP promoter activity was determined by luciferase assay and is expressed as fold increase in luciferase activity. Each experiment was performed in duplicate. In (**c** and **f–h**) mean + S.E.M. of three independent experiments is shown; *$P < 0.05$; **$P < 0.01$; n.s., not significant
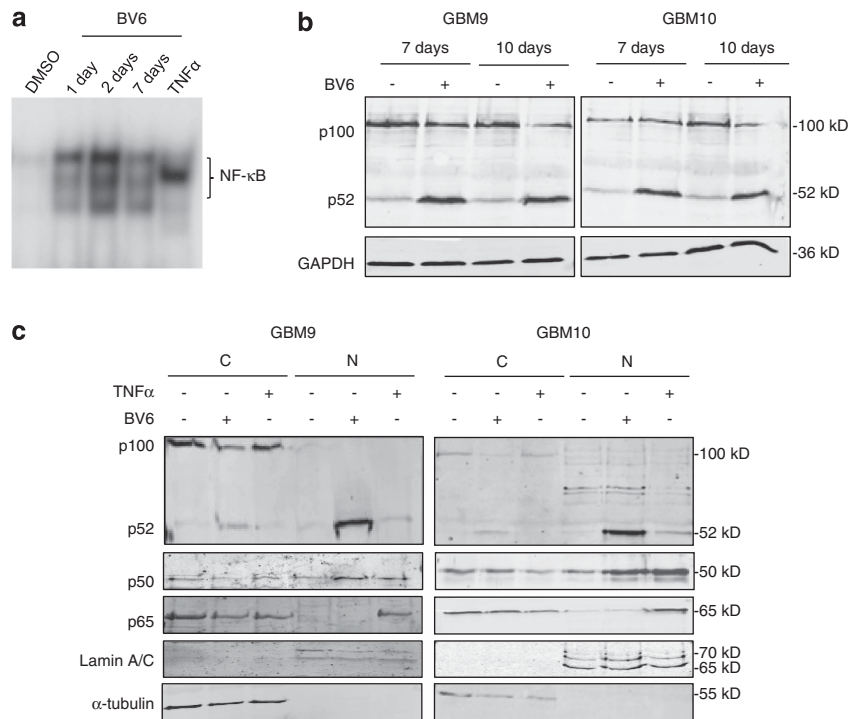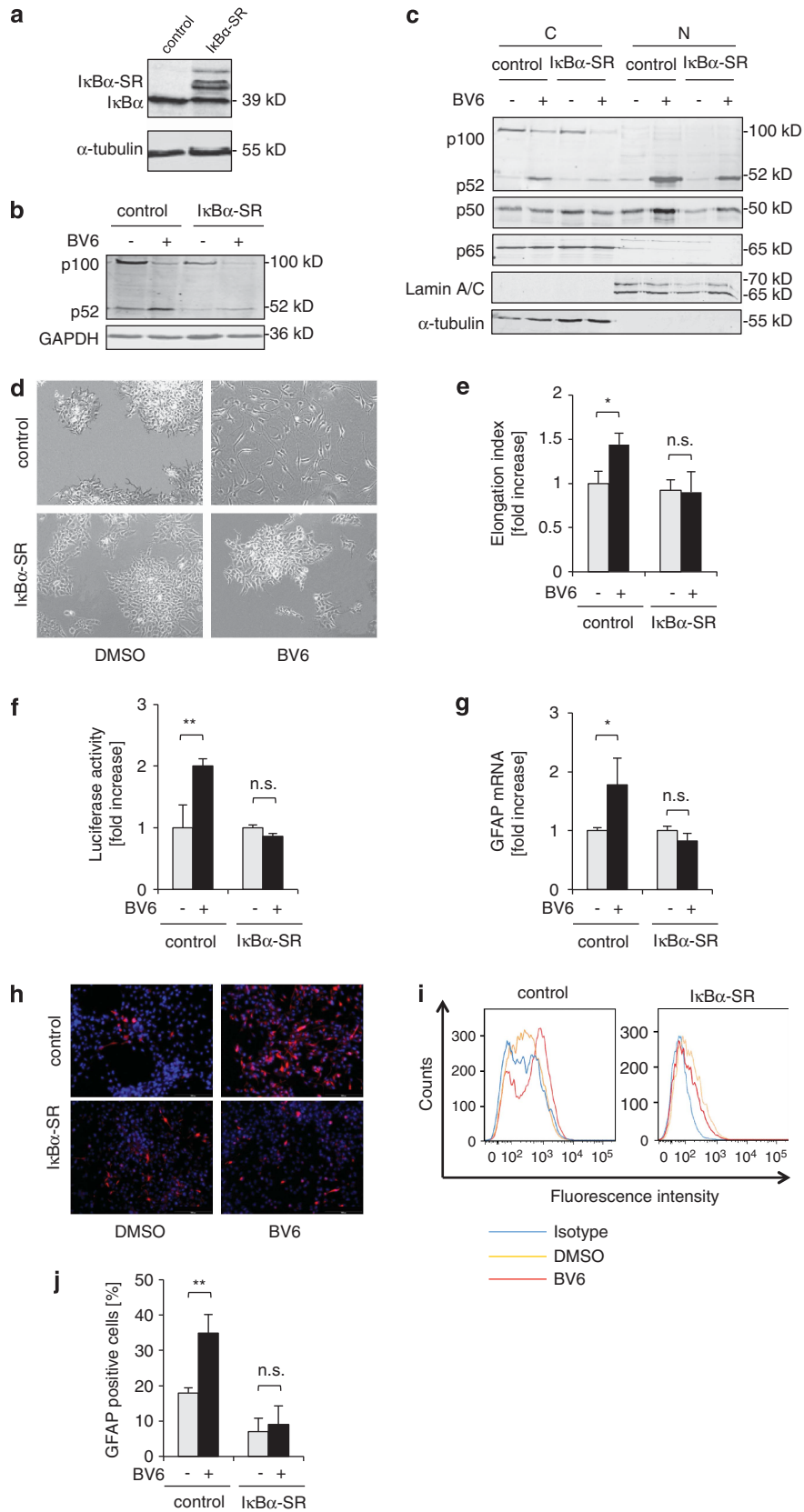
Figure 3 Smac mimetic activates the NF-κB pathway. (**a**) GBM10 cells were treated for indicated times with 1 μM BV6 or DMSO; stimulation with 10 ng/ml TNFα for 1 hour was used as positive control. Nuclear extracts were analyzed for NF-κB DNA-binding activity by EMSA. A representative experiment of two experiments is shown. (**b**) GBM CSLCs were treated for indicated times with BV6 (GBM9: 0.6 μM, GBM10: 1 μM BV6) or DMSO. Expression levels of p100 and p52 were analyzed by western blotting. Expression level of GAPDH served as loading control. (**c**) GBM CSLCs were treated for 7 days with BV6 (GBM9: 0.6 μM, GBM10: 1 μM BV6) or DMSO; stimulation with 10 ng/ml TNFα for 1 hour was used as positive control. Expression levels of p100, p52, p65 and p50 were analyzed in cytoplasmic (C) and nuclear (N) fractions by western blotting. α-tubulin served as purity and loading control for cytoplasmic fractions and lamin A/C for nuclear fractions

p100 (Figure 4b), consistent with the notion that p100 is a NF-κB target gene,[28] and reduced BV6-stimulated processing of p100 to p52 (Figures 4b and c), further demonstrating that IκBα-SR blocks NF-κB signaling in GBM CSLCs. Of note, NF-κB inhibition prevented the BV6-induced cell elongation compared with vector control cells (Figures 4d and e). Importantly, NF-κB inhibition abolished the BV6-stimulated increase in GFAP transcriptional activity, GFAP mRNA levels and GFAP protein expression (Figures 4f–j, Supplementary Figure S5C). These experiments demonstrate that NF-κB activation is required for BV6-induced transcriptional upregulation of GFAP expression and astrocytic differentiation of GBM CSLCs. To investigate whether TNFR1/TNFα signaling is involved in BV6-mediated differentiation of GBM CSLCs, we knocked down TNFR1. Silencing of TNFR1 did not significantly alter the BV6-mediated increase in GFAP protein levels and had no effect on cell viability (Supplementary Figure S6), pointing to a TNFR1/TNFα-independent mechanism.

Smac mimetic decreases stem cell markers in GBM CSLCs. As one hallmark of differentiation is the loss of stem cell markers, we next asked whether BV6-stimulated differentiation modulates the expression of stem cell markers. To address this question, we analyzed expression levels of nestin, CD133, Sox2 and Nanog. Importantly, BV6 significantly decreased mRNA levels of CD133, Sox2 and Nanog in GBM CSLCs (Figure 5a). In parallel,

BV6 significantly reduced surface expression of CD133 protein in GBM9 and GBM10 cells, whereas it did not change CD133 protein expression in NSCs (Figures 5b and c). Control experiments using 2% FCS to induce stem cell differentiation showed that exposure to FCS significantly reduced mRNA levels of all four stem cell markers in GBM10 cells (Figure 5a) and also decreased the number of CD133-positive cells in NSCs (Supplementary Figures S7A and B). By comparison, BV6 did not change mRNA or protein expression of nestin in GBM9, GBM10 and NSCs (Figures 5a and d). To control that the culture conditions as monolayer do not modify CD133 expression of NSCs, we also compared the abundance of CD133-positive cells after 7 days of monolayer and sphere culture. The percentage of CD133-positive NSCs was similar for monolayer and sphere cultures (Supplementary Figures S7C and D), demonstrating that monolayer culture does not alter the percentage of CD133-positive NSCs. Together, these findings demonstrate that BV6 decreases the expression of several stem cell markers in GBM CSLCs.

Various IAP inhibitors stimulate cell elongation, enhance astrocytic differentiation and reduce stem cell markers of GBM CSLCs. To further explore whether inhibition of IAP proteins regulates differentiation of GBM CSLCs, we used two additional, structurally different pharmacological IAP inhibitors that antagonize cIAP1, cIAP2 and XIAP.[29–31] IAP inhibitors 2 and 3 at a subtoxic

a

IκBα-SR
IκBα ·····- 39 kD

α-tubulin - 55 kD

b

control   IκBα-SR
BV6   -   +   -   +
p100 ·····-100 kD
p52 - 52 kD
GAPDH - 36 kD

c

C   N
control IκBα-SR control IκBα-SR
BV6   -   +   -   +   -   +   -   +
p100 ·····-100 kD
p52 - 52 kD
p50 - 50 kD
p65 - 65 kD
Lamin A/C - 70 kD
- 65 kD
α-tubulin - 55 kD

d

e

f

g

h

i

— Isotype
— DMSO
— BV6

j

concentration, which caused downregulation of cIAP1, cIAP2 and XIAP and processing of p100 to p52, triggered a significant increase in cell elongation, promoted astrocytic differentiation and significantly decreased stem cell markers of GBM CSLCs (Supplementary Figure S8).

Smac mimetic reduces clonogenicity of GBM CSLCs *in vitro* and *in vivo*. Differentiation of GBM CSLCs has been associated with a reduction of stemness properties such as clonogenicity.[9] Therefore, we next tested whether treatment with BV6 alters the clonogenic potential of GBM CSLCs. To this end, GBM9 and GBM10 cells were treated with BV6 and then cultivated in suspension in stem cell medium at a density of 10 000 cells/ml to monitor neurosphere formation or, alternatively, at decreasing dilutions for *in vitro* limiting dilution assay. Of note, pretreatment with BV6 reduced the ability of GBM CSLCs to form neurospheres (Figure 6a) and significantly decreased their clonogenic potential (Figure 6b).

To test whether treatment with BV6 alters *in vivo* clonogenicity, GBM9 cells were treated with BV6 or DMSO and then injected at decreasing dilutions either orthotopically in the corpus callosum or subcutaneously in the right side of athymic nude mice. Depending on the number of cells injected, BV6 treatment reduced tumor formation in both *in vivo* models (Tables 1 and 2). In the intracranial model, a marked difference in tumor formation between BV6- and DMSO-treated cells was observed for 100 000 and 10 000 cells injected (Table 1). In the subcutaneous model, BV6-treated cells formed less tumors than DMSO-treated cells for 500 000 ($P < 0.05$) and 100 000 (n.s.) cells injected (Table 2). Together, these data demonstrate that BV6 reduces the clonogenic potential of GBM CSLCs *in vitro* as well as *in vivo*.

Smac mimetic reduces tumorigenicity of GBM CSLCs *in vivo* and increases survival. To evaluate the ability of BV6-treated GBM CSLCs to form a tumor *in vivo* we used an orthotopic and a subcutaneous GBM model in nude mice to test whether treatment with BV6 decreases the tumorigenic potential of GBM CSLCs. Of note, treatment with BV6 reduced tumor formation in both GBM models (Tables 1 and 2). Importantly, BV6 also significantly increased the survival of mice (Figures 7a–c). Analysis of astrocytic differentiation (using GFAP staining), proliferation (using Ki67 staining) and

apoptosis (using caspase-3 staining) showed a tendency towards increased astrocytic differentiation and decreased proliferation in the BV6-treated group, whereas no difference in apoptosis was observed (Table 1, Figure 7d). Together, this set of experiments demonstrates that BV6 reduces tumorigenicity of GBM CSLCs *in vivo* and significantly increases survival of mice.

Discussion

IAP proteins have been described to regulate signal transduction pathways beyond apoptosis.[15] In this study, we identify a novel non-apoptotic role of the Smac mimetic BV6 in the regulation of GBM CSLCs differentiation. We demonstrate for the first time that BV6 at a sublethal concentration induces astrocytic differentiation of GBM CSLCs in a NF-κB pathway-dependent manner resulting in reduced clonogenicity and tumorigenicity of GBM CSLCs *in vivo*. Several lines of evidence support this conclusion. First, BV6 triggers differentiation of GBM CSLCs towards the astrocytic lineage as shown by an increase in the astrocytic marker protein GFAP, whereas expression of the neuronal marker β-III-tubulin does not change. BV6 stimulates astrocytic differentiation via enhanced transactivation of the GFAP promoter, as demonstrated by increased GFAP transcriptional activity and elevated GFAP mRNA and protein levels. This BV6-stimulated increase in differentiation is accompanied by a decrease in stem cell markers like CD133, Sox2 and Nanog. In contrast to GBM CSLCs, BV6 does not alter differentiation or stemness characteristics of NSCs pointing to a differential effect of BV6 on malignant GBM CSLCs *versus* non-malignant NSCs. Second, BV6 activates NF-κB signaling in GBM CSLCs, as it triggers proteolytic processing of p100 to p52, translocation of p52 and p50 into the nucleus and increased NF-κB DNA-binding. NF-κB activation is required for BV6-induced astrocytic differentiation, as inhibition of NF-κB by overexpression of IκBα-SR blocks the BV6-stimulated increase in cell elongation, GFAP transcriptional activity, and GFAP protein and mRNA levels. Third, treatment with BV6 reduces clonogenicity of GBM CSLCs *in vitro* and *in vivo*, suppresses their tumorigenicity in orthotopic and subcutaneous mouse models and significantly increases the survival of mice. Together, these data underscore the requirement of BV6-stimulated NF-κB activation to mediate astrocytic differentiation of GBM CSLCs.

Figure 4 Smac mimetic-induced astrocytic differentiation is blocked in IκBα-SR cells. (**a**) GBM10 cells were transduced with IκBα-SR or vector control and were analyzed for expression of IκBα by western blotting. α-tubulin expression served as a loading control. (**b**) GBM10 cells stably expressing IκBα-SR or vector control were treated for 7 days with 1 μM BV6 or DMSO. Expression levels of p100 and p52 were analyzed by western blotting. Expression of GAPDH served as loading control. (**c**) GBM10 cells stably expressing IκBα-SR or vector control were treated for 7 days with 1 μM BV6 or DMSO. Expression levels of p100, p52, p65 and p50 were analyzed in cytoplasmic (C) and nuclear (N) fractions by western blotting. α-tubulin served as purity and loading control for cytoplasmic fractions and lamin A/C for nuclear fractions. (**d** and **e**) GBM10 cells stably expressing IκBα-SR or vector control were treated for 7 days with 1 μM BV6 or DMSO. Cell morphology was analyzed by phase-contrast microscope; scale bar, 500 μm. A representative experiment of three experiments is shown (**d**). Cell elongation was quantified by measuring cell length and width and by calculating cell elongation index (length/width); fold increase in cell elongation is shown (**e**). (**f**) GBM10 cells stably expressing IκBα-SR or vector control were treated for 7 days with 1 μM BV6 or DMSO. GFAP promoter activity was determined by luciferase assay. (**g**) GBM10 cells stably expressing IκBα-SR or vector control were treated for 7 days with 1 μM BV6 or DMSO. GFAP mRNA levels were analyzed by quantitative RT-PCR and fold increase in GFAP mRNA levels is shown. (**h**) GBM10 cells stably expressing IκBα-SR or vector control were treated for 7 days with 1 μM BV6 or DMSO. Cells were then fixed and stained with anti-GFAP antibody and counterstained with DAPI. Representative pictures of three independent experiments are shown. Scale bar, 500 μm. (**i** and **j**) GBM10 cells stably expressing IκBα-SR or vector control were treated for 7 days with 1 μM BV6 or DMSO. Cells were dissociated and stained with anti-GFAP antibody and isotype control for FACs analysis (**i**). The percentage of CD133-positive cells is presented (**j**). Mean + S.E.M. of three independent experiments is shown. In (**e–g**) mean + S.E.M. of three independent experiments performed in duplicate (**f**) or triplicate (**e** and **g**) is shown; *$P < 0.05$; **$P < 0.01$; n.s., not significant
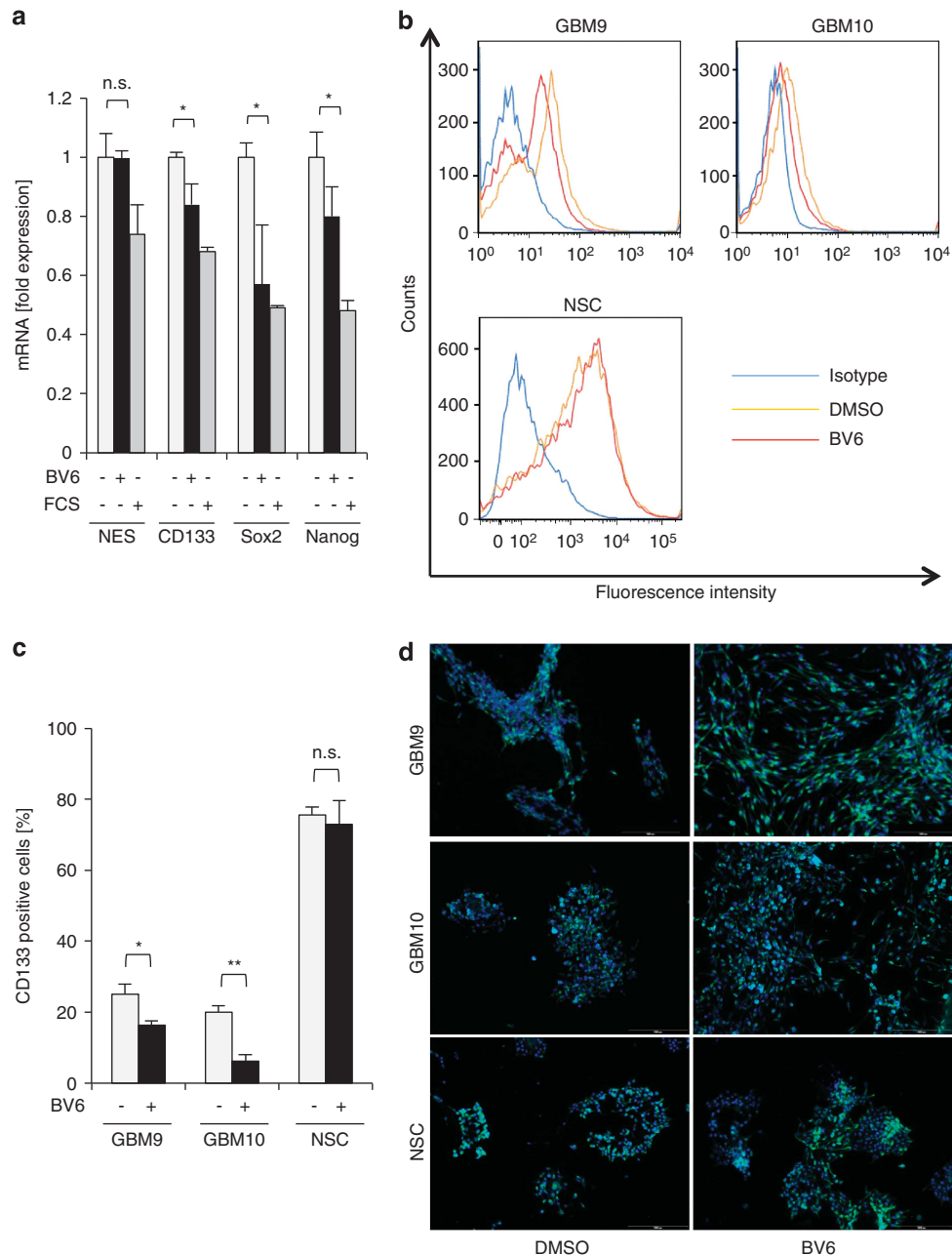
a

b

c

d

Figure 5 Smac mimetic decreases stem cell markers. (**a**) GBM10 cells were treated with 1 μM BV6 or 2% FCS for 7 days or DMSO was used as solvent. mRNA levels of nestin (NES), CD133, Sox2 and Nanog were analyzed by quantitative RT-PCR and results are presented as fold increase of DMSO-treated cells. Mean + S.E.M. of three independent experiments performed in triplicate is shown. (**b** and **c**) GBM9 cells were treated for 10 days with 0.6 μM BV6 or DMSO; GBM10 and NSCs for 7 days with 1 μM BV6 or DMSO. Cells were dissociated and stained with anti-CD133-PE antibody or with isotype control for FACS analysis. A representative experiment from three independent experiments is shown (**b**). The percentage of CD133-positive cells with mean + S.E.M. of three independent experiments is shown (**c**); *P<0.05; **P<0.01; n.s., not significant. (**d**) GBM9 cells were treated for 10 days with 0.6 μM BV6 or DMSO; GBM10 and NSCs for 7 days with 1 μM BV6 or DMSO. Then, cells were fixed and stained with anti-nestin antibody and counterstained with DAPI. Representative pictures of four independent experiments are shown; scale bar, 500 μm

The novelty of our study relates in particular to the identification of a non-apoptotic function of the Smac mimetic BV6 as an inducer of GBM CSLCs differentiation into the astrocytic lineage, which is driven by NF-κB. Smac mimetic-stimulated NF-κB signaling likely involves canonical and non-canonical NF-κB pathways. The critical role of NF-κB in mediating differentiation by BV6 is underscored by the ectopic expression of dominant-negative IκBα-SR, which blocks

BV6-stimulated transcriptional activation of GFAP, upregulation of GFAP mRNA and protein levels as well as differentiation. Interestingly, a conserved NF-κB binding site within the GFAP promoter has been described, suggesting that GFAP is a NF-κB target gene.[32] In line with our results, inhibition of NF-κB by IκBα-SR was demonstrated to suppress GFAP expression.[32]

NF-κB has previously been implicated in regulating differentiation of normal and malignant cells of the central
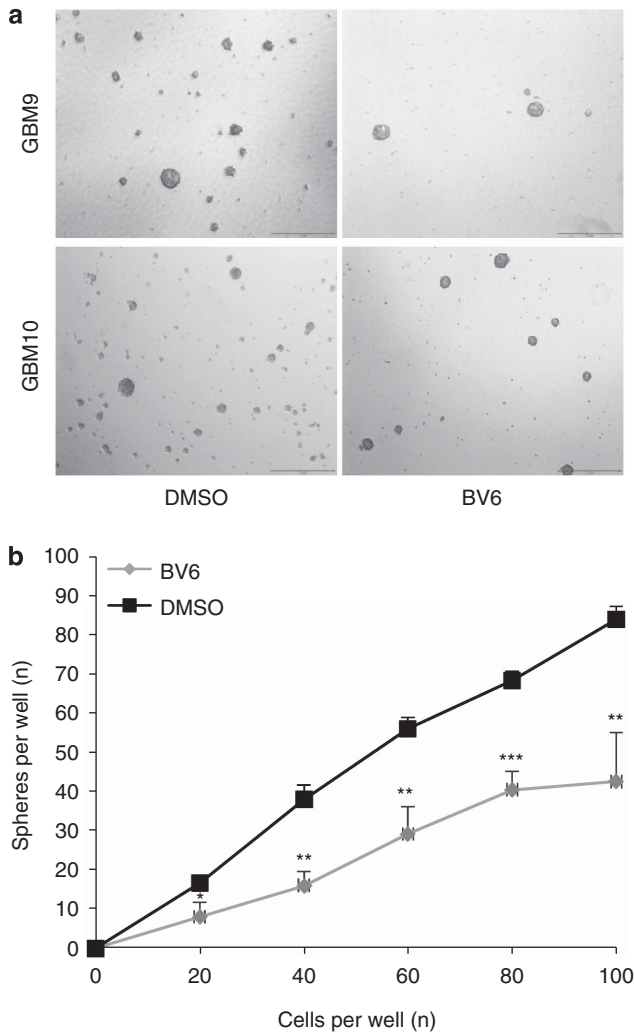
Figure 6 Smac mimetic reduces clonogenicity of GBM CSLCs. (**a**) GBM9 cells were treated for 10 days with 0.6 μM BV6 or DMSO and GBM10 cells for 7 days with 1 μM BV6 or DMSO. After treatment, cells were detached from the plate and were cultured as stem cell culture to assess sphere formation. Representative phase-contrast pictures from three independent experiments after 7 days of stem cell culture are shown, scale bar, 500 μm. (**b**) GBM9 cells were treated for 10 days with 0.6 μM BV6 or DMSO. After treatment, cells were detached from the plate and seeded at decreasing dilutions (100, 80, 60, 40, 20 and 1 cells per well) in a 96-well plate. After 1 week, the number of spheres per well was counted and plotted against the number of cells seeded per well. Mean + S.E.M. of three independent experiments is shown; *$P<0.05$; **$P<0.01$; ***$P<0.001$

Table 1 Smac mimetic reduces clonogenicity and tumorigenicity of GBM CSLCs in an intracranial mouse model *in vivo*

Treatment	Number of cells injected	Tumor formation (%)	GFAP staining (%)	Ki67 staining (%)	Caspase-3 staining (%)
BV6	500 000	100 (8/8)	27 ± 3	32 ± 6	26 ± 9
	100 000	62.5 (5/8)	24 ± 9	40 ± 3	50 ± 6
	10 000	50 (4/8)	16 ± 5	27 ± 11	27 ± 3
DMSO	500 000	100 (7/7)	22 ± 5	40 ± 4	41 ± 8
	100 000	100 (8/8)	9 ± 4	52 ± 6	40 ± 6
	10 000	100 (8/8)	13 ± 4	37 ± 4	23 ± 2

GBM9 cells were treated for 10 days with 0.6 μM BV6 or DMSO. After treatment, cells were detached from the plate and 500 000, 100 000 or 10 000 cells were injected into the corpus callosum of athymic nude mice. The percentage of tumor formation validated by histological analysis (H&E staining) and the percentage of GFAP, Ki67 and caspase-3-positive cells ± S.E.M. are listed

Table 2 Smac mimetic reduces clonogenicity and tumorigenicity of GBM CSLCs in an subcutaneous mouse model *in vivo*

Treatment	Cells injected (*n*)	Tumor formation (%)	Time between injection and tumor formation (days)
BV6	500 000	40 (2/5)*	56–70
	100 000	0 (0/5)	No tumor formation
	10 000	0 (0/5)	No tumor formation
DMSO	500 000	80 (4/5)	28–42
	100 000	60 (3/5)	70–105
	10 000	0 (0/5)	No tumor formation

GBM9 cells were treated for 10 days with 0.6 μM BV6 or DMSO. After treatment, cells were detached from the plate and 500 000, 100 000 or 10 000 cells were injected on the right side of athymic nude mice. The percentage of tumor formation validated by histological analysis (H&E staining) and the time between tumor injection and tumor formation are listed; *$P<0.05$

nervous system. Glioblastoma-initiating cells undergoing differentiation were reported to activate NF-κB with increased nuclear translocation of the p65 NF-κB subunit and enhanced binding of p65 and p50 to the DNA.[33] Although these results point to activation of the canonical NF-κB pathway, the question whether or not canonical *versus* non-canonical NF-κB is involved in controlling differentiation of glioblastoma-initiating cells was not specifically addressed in that study.[33] Blockade of NF-κB accelerated the differentiation of glioblastoma-initiating cells towards a neuronal lineage with reduced astrocytic differentiation, underlining the fact that NF-κB activity is required for differentiation into astrocytes.[33]

Furthermore, Dexamethasone was described to block astroglial differentiation from mesencephalic neural precursor cells by suppressing activation of the NF-κB pathway.[34] The small-molecule NF-κB inhibitor SN50 recapitulated this effect of Dexamethasone, indicating that Dexamethasone prevents astroglial differentiation of neural precursors by inhibiting NF-κB.[34] In addition, ionizing radiation was reported to stimulate astrocyte differentiation of NSCs by activating NF-κB in cells that survived radiation treatment.[35]

Besides controlling astrocytic differentiation, the NF-κB pathway has also been implicated in the differentiation of other cell types, for example, myeloid cells and osteoclasts.[29,36] Accordingly, components of the non-canonical NF-κB pathway such as NF-κB2/RelB were shown to be necessary for differentiation of CD34 + hematopoietic stem/progenitor cells into the myeloid lineage, as siRNA-mediated knockdown of NF-κB2 decreased the percentage and the size of myeloid colonies derived from CD34 + hematopoietic stem/progenitor cells.[36] Also, the alternative NF-κB pathway was reported to be required during osteoclastogenesis for the differentiation of osteoclast precursors, as the ability of NIK-deficient osteoclast precursors to differentiate was restored by overexpression of RelB, but could not be compensated for by p65.[29] Recently, loss of cIAP1 protein resulting in NF-κB
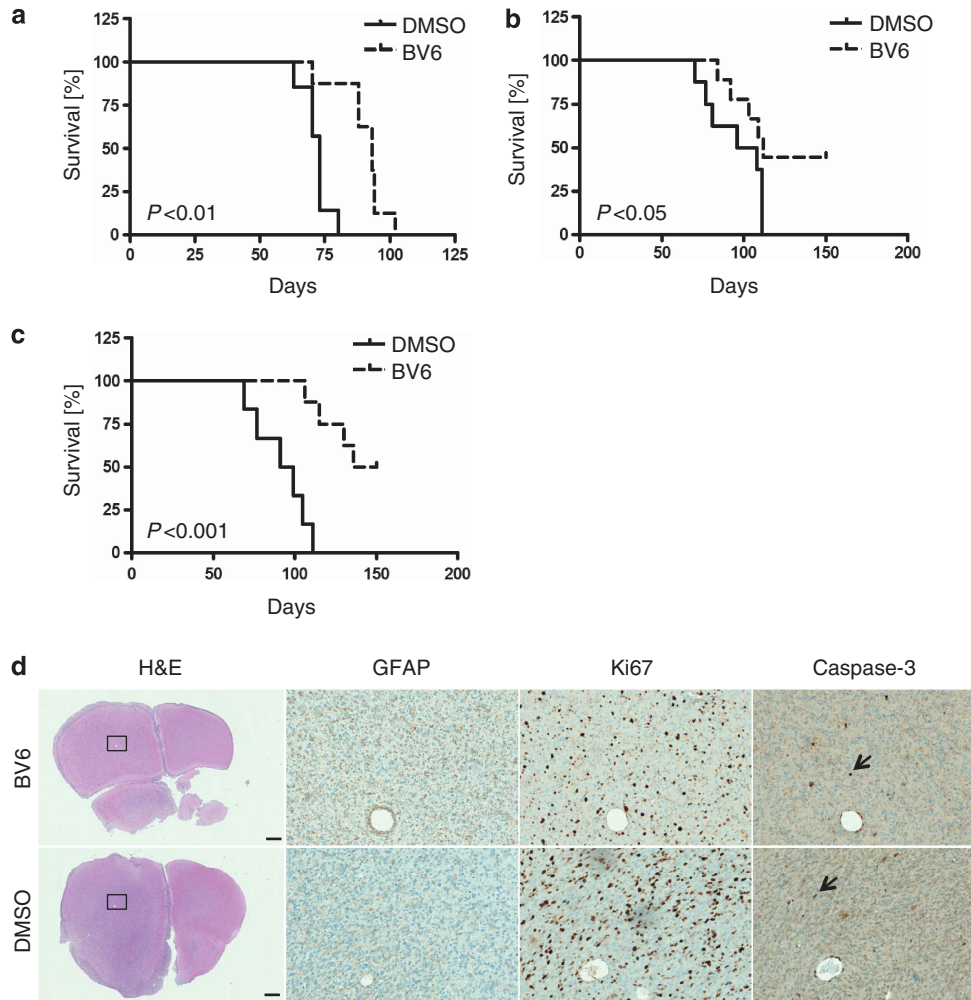
Figure 7 Smac mimetic reduces tumorigenicity of GBM CSLCs *in vivo* and increases survival of mice. (**a–c**) GBM9 cells were stereotactically injected after treatment with 0.6 μM BV6 or DMSO for 10 days at decreasing dilutions (**a**: 500 000 cells, eight mice were injected with BV6-treated cells and seven mice with DMSO-treated cells; **b**: 100 000 cells, eight mice per condition; **c**: 10 000 cells, eight mice per condition) into the corpus callosum of athymic nude mice. Overall survival curves of mice were estimated by the Kaplan–Meier method. (**d**) Representative H&E, GFAP, Ki67 and caspase-3 stainings of tumors derived from BV6- and DMSO-treated GBM9 cells are shown. Scale bars (500 μm) are shown for H&E stainings; GFAP, Ki67 and caspase-3 stainings correspond to sixfold magnification of the black square located on the H&E stainings. Black arrows highlight apoptotic cells; see also Table 1

activation, preferentially non-canonical NF-κB signaling, was shown to promote myoblast fusion.[37]

Furthermore, IAP proteins have been implied as regulators of differentiation. For example, differentiation of human prostate epithelial cells was described to be accompanied by downregulation of cIAP1 and XIAP mRNA and protein levels.[25] During hematopoietic differentiation, cIAP1 was shown to translocate from the nucleus to the Golgi, pointing to an involvement of cIAP1 in cellular differentiation.[24] Further, depletion of IAP proteins was reported to trigger maturation of immature dendritic cells, as treatment with BV6 resulted in upregulation of differentiation markers.[30]

Besides differentiation, NF-κB has been shown to control proliferation of NSCs.[38] Also, inhibition of NF-κB in glioblastoma-initiating cells was demonstrated to promote growth arrest and senescence.[33] By comparison, in our present study we found no evidence showing that Smac

mimetic alters cell proliferation via activation of NF-κB, in line with a context-dependent function of NF-κB in the control of differentiation and proliferation. This differential regulation of proliferation or differentiation by NF-κB has been linked to distinct phases of the cell cycle in which NF-κB acts: in the G1-phase, NF-κB was shown to activate cyclin D1 expression, which promotes G1-to-S progression, whereas in the M-phase, NF-κB was described to trigger differentiation.[39,40] Interestingly, NF-κB has also been implicated in controlling survival, proliferation and differentiation of normal and malignant stem cells by altering, for example, the expression of pluripotency genes such as Nanog.[41,42] As we found a decline in several stem cell markers including Nanog upon BV6-stimulated differentiation, it will be interesting to determine whether this BV6-mediated decrease is caused directly by NF-κB or indirectly via the induction of differentiation. In contrast to GBM CSLCs, BV6 does not alter differentiation or stemness characteristics of NSCs, pointing

to a differential effect of BV6 on malignant GBM CSLCs *versus* non-malignant NSCs.

Our findings will likely have important implications for the use of Smac mimetics as cancer therapeutics, because BV6-stimulated differentiation results in impaired ability of GBM CSLCs to form colonies *in vitro* and to grow as a tumor *in vivo*. As induction of differentiation represents a therapeutic strategy to target GBM CSLCs, inhibition of IAP proteins may offer new opportunities in the context of differentiation therapies. The relevance of targeting the glioblastoma population with cancer stem cell properties is underscored by a recent report showing that glioma cancer stem cells sustain long-term tumor growth after chemotherapy.[7] Furthermore, we previously reported that inhibition of IAP proteins by Smac mimetic can prime GBM cells for TRAIL-, chemotherapy- or irradiation-induced apoptosis.[21,22,43,44] The notion that Smac mimetic can exert non-apoptotic functions under certain conditions is supported by our recent findings showing that Smac mimetics can promote migration and invasion of GBM cells at a non-lethal concentration.[45] As tumor heterogeneity comprising CSLCs as well as more mature GBM cells is a characteristic feature of GBM, Smac mimetics may support migration/invasion or differentiation within the same tumor, depending, for example, on the cell type.

In conclusion, by identifying and characterizing a novel non-apoptotic role of the Smac mimetic BV6 in the regulation of GBM CSLCs differentiation, our findings provide novel insights into the biological activities of Smac mimetics, which open new perspectives for their use as cancer therapeutics.

Materials and Methods

Cell culture and chemicals. GBM CSLCs were characterized and cultured in serum-free medium as described previously.[26] Briefly, cells were cultivated in suspension in DMEM/F12 medium supplemented with 5 μg/ml insulin, 0.1 mM putrescin, 100 μg/ml transferrin, 2.10^{-8} M progesterone (all purchased from Sigma, Deisenhofen, Germany), 50 mg/ml penicillin/streptomycin (Invitrogen, Heidelberg, Germany) and growth factors including B27 (Invitrogen), 20 ng/ml epidermal growth factor (EGF, R&D Systems, Inc., Wiesbaden, Germany) and 10 ng/ml basic fibroblast growth factor (bFGF, Sigma). NSCs were recently characterized and cultured as described.[27] The T98G glioblastoma cell line was obtained from ATCC (Manassas, VA, USA) and used as a positive control for cIAP2 expression. Cells were seeded after sphere dissociation on 10 μg/ml poly-DL-ornithine hydrobromide (Sigma)-coated plates. The bivalent Smac mimetic BV6[23] was a kind gift from Genentech Inc. (San Francisco, CA, USA). BV6 was added once in the beginning of the experiments. FCS was purchased from Invitrogen and TNFα from Biochrom (Berlin, Germany). All other chemicals were obtained from Sigma unless indicated otherwise.

Determination of cell viability. Cell viability was assessed by 3-(4,5-dimethylthiazol-2-yl)-2,5-diphenyltetrazolium bromide (MTT) assay according to the manufacturer's instructions (Roche Diagnostics, Mannheim, Germany).

Western blots. Western blot analysis was performed as described previously[46] using the following antibodies: anti-cIAP1 (R&D Systems, Inc.), anti-cIAP2 (Epitomics, Burlingame, CA, USA), anti-XIAP (BD Biosciences, Franklin Lake, NJ, USA), anti-caspase-3, anti-IκBα (Cell Signaling, Beverly, MA, USA), anti-β-actin (Sigma), anti-α-tubulin (Calbiochem, Darmstadt, Germany), anti-p50 and anti-p65 from Santa Cruz Biotechnology (Santa Cruz, CA, USA), anti-p52 (Millipore, Schwalbach, Germany) and anti-lamin A/C (Novocastra, Berlin, Germany). Donkey anti-mouse IgG, donkey anti-rabbit IgG or donkey anti-goat IgG were used for fluorescence detection at 700 nm and/or 800 nm (LI-COR Biotechnology, Bad Homburg, Germany). Caspase-3 was immunodetected by enhanced chemoluminescence (Amersham Biosciences, Freiburg, Germany) using anti-rabbit IgG-HRP secondary antibody (Santa Cruz Biotechnology).

Nuclear extractions and EMSA. Nuclear extracts were prepared as previously described.[47] Shortly, cells were washed, scraped and collected by centrifugation at 2500 r.p.m. for 5 minutes at 4 °C. Cells were resuspended in low-salt buffer, lysed for 15 min on ice, followed by addition of a 10% Igepal CA-630 solution and centrifugation. The pelleted nuclei were resuspended in high-salt buffer and nuclear supernatants were obtained by centrifugation. DNA-binding activity of NF-κB was analyzed by EMSA and the following sequence was used as specific oligomer for NF-κB: 5′-AGTTGAGGGGACTTTCCCAGGC-3′ (sense). Single-stranded oligonucleotides were labeled with γ-[32P]-ATP by T4-poly-nucleotide kinase (MBI Fermentas GmbH, St. Leon-Rot, Germany), annealed to the complementary oligomer strand and purified on sephadex columns (Illustra Nick Columns, GE Healthcare, Piscataway, NJ, USA). Binding reactions containing 5 μg nuclear extract, 1 μg Poly(dI:dC) (Sigma), labeled oligonucleotide (10 000 cpm) and 5 × binding buffer were incubated for 30 min on ice. Binding complexes were resolved by electrophoresis in non-denaturing 6% polyacrylamide gels using 0.5 × TBE as running buffer and assessed by autoradiography.

Immunofluorescence staining. Cells were grown in Labtek chamber slides (BD Biosciences, Heidelberg, Germany), fixed with 4% paraformaldehyde and permeabilized with 0.1% Triton-100X for 10 minutes. Primary antibodies against nestin (mouse IgG, 5 μg/ml, Abcam, Cambridge, UK), glial fibrillary acidic protein (GFAP, rabbit IgG, 10 μg/ml, Dako) and β-III-tubulin (mouse IgG, 2 μg/ml, Covance, Denver, PA, USA) were incubated overnight at 4 °C. Secondary antibodies, Texas-red Goat anti-rabbit IgG (H + L) and FITC Goat anti-mouse IgG (H + L) were purchased from Jackson Immunoresearch (Newmarket, UK), and were incubated for 1 hour at room temperature in the presence of DAPI for nuclear staining. All the images were obtained using an Olympus IX71 microscope (Olympus, Hamburg, Germany).

Flow cytometry. CD133-PE (CD133/2) antibody was purchased by Miltenyi Biotec (Bergisch Gladbach, Germany); staining was performed as previously described.[26] Staining for GFAP and β-III-tubulin was performed as follows: cells were harvested, fixed on ice in 2% paraformaldehyde for 20 min, permeabilized with 0.1% Triton-100X for 20 min on ice and incubated for 30 min on ice with primary antibodies (50 μg/ml GFAP, 10 μg/ml β-III tubulin) followed by the respective secondary antibodies. Isotype controls were used as negative controls (mouse IgG2a-PE, Miltenyi Biotec; rabbit IgG-PE, eBioscience, Frankfurt, Germany; mouse IgG2b-FITC, Miltenyi Biotec). Cells were processed on a FACSCanto II (Becton Dickinson, Heidelberg, Germany). Data were analyzed using FlowJo software (Tree Star, Inc., Ashland, OR, USA).

Quantitative RT-PCR. Total RNA was extracted using peqGOLD Total RNA kit from Peqlab Biotechnologie GmbH (Erlangen, Germany) according to the manufacturer's instructions. Total RNA (2 μg) was used to synthesize the corresponding cDNA using RevertAid H Minus First Strand cDNA Synthesis Kit (MBI Fermentas GmbH). To quantify gene expression levels, SYBR-Green based qRT-PCR was performed using the 7900HT fast real-time PCR system from Applied Biosystems (Darmstadt, Germany). Data were normalized on 18S-rRNA expression as reference gene. Primers are listed in Supplementary Table 1. Melting curves were plotted to verify the specificity of the amplified products. All determinations were performed in triplicate. The relative expression of the target gene transcript and reference gene transcript was calculated as $\Delta\Delta C_t$. Two independent experiments were performed for each gene.

Luciferase assay. Cells were plated on poly-DL-ornithine coated 12-well plates as described above. The day after, cells were transfected with the luciferase construct GF1L containing the mouse GFAP promoter that was previously described[48] and kindly provided by Professor K Nakashima (Ikoma, Japan) and renilla luciferase vector using Fugene HD (Roche Diagnostics). The day after transfection, cells were stimulated with BV6. Five days after stimulation, cells were lysed and luciferase activity was determined by the Dual-Luciferase Reporter Assay System (Promega, Madison, WI, USA) and a microplate reader (TECAN Infinite M200, Crailsheim, Germany) according to the manufacturer's instructions. Firefly luciferase values were normalized to *Renilla* luciferase values.

Retroviral transduction. Overexpression of the dominant-negative IκBα superrepressor (IκBα-SR) was performed by retroviral transduction using the pCFG5-IEGZ retroviral vector system as previously described.[49] Knockdown of

TNFR1 was performed by lentiviral shRNA vectors as previously described[45] using pGIPZ-shRNAmir-vectors from Thermo Fisher Scientific (Dreieich, Germany; non-silencing control RHS4346, TNFR1 shRNA RHS4430-101170340).

Limiting dilution assay. GBM9 cells were treated with $0.6\,\mu$M BV6 or DMSO. After 10 days, cells were detached, dissociated and plated on 96-well plates at decreasing dilutions (100, 80, 60, 40, 20 and 1 cells per well). After 1 week, the number of spheres per well was counted and plotted against the number of cells seeded per well.

***In vivo* GBM mouse models.** For the orthotopic GBM model, GBM9 cells were injected stereotactically at decreasing dilutions (500 000, 100 000 and 10 000 cells) into the corpus callosum of 6-week-old athymic *nude* mice (Harlan France, Gannat, France) after treatment for 10 days with $0.6\,\mu$M BV6 or DMSO. The injection coordinates were 1 mm anterior to bregma, -1 mm lateral and 2 mm in deep from the cortex. Animals were anesthetized prior to all procedures and were observed until full recovery. Mice were killed as soon as they started to develop clinical symptoms (ataxia and loss of weight) and their brains were immediately removed and fixed in 4% formalin for 24 h before being embedded in paraffin. Experimental protocols including animals were reviewed and approved by the Institutional Animal Care Committee of the School of Medicine at Marseille.

For the subcutaneous GBM model, GBM9 cells were injected at decreasing dilutions (500 000, 100 000 and 10 000 cells) in the right side of 6-week-old athymic *nude* mice (Harlan France) after treatment for 10 days with $0.6\,\mu$M BV6 or DMSO. Mice were killed when the tumor reached a diameter of 1.5 cm. Experimental protocols including animals were reviewed and approved by the Institutional Animal Care Committee of the School of Medicine at Marseille.

Immunohistochemistry. H&E staining was performed on $5\,\mu$m sections of formalin-fixed paraffin-embedded mouse brains for tumor detection. In cases of tumor formation, immunostainings for GFAP (Clinisciences, Nanterre, France), Ki67 (Dako, Trappes, France) and caspase-3 (BD Biosciences, Le Pont de Claix, France) were performed using a Ventana automate (Benchmark, Ventana Medical Systems SA, Illkirch, France). In each case, steam heat-induced antigen retrieval was performed. The percentage of GFAP-, Ki67- or caspase-3 positive cells was determined by counting 500 cells per slide in high-power fields on five different slides for each tumor corresponding to five different areas of the tumors and an average of each area was done in order to obtain a representative percentage. Only clear and strong stainings were counted as positive.

Statistical analysis. Statistical significance was assessed by two-sided Student's *t*-test using Microsoft Excel (Microsoft Deutschland GmbH, Unterschleißheim, Germany). Mann–Whitney *U*-test and Fisher's exact test were used to test the significance of immunostainings and tumor formation in mouse models, respectively. Overall survival curves of mice were estimated by the Kaplan–Meier method (GraphPad Prism4, GraphPad Software, Inc., La Jolla, CA, USA).

Conflict of Interest

The authors declare no conflict of interest.

1. Louis DN, Ohgaki H, Wiestler OD, Cavenee WK, Burger PC, Jouvet A *et al.* The 2007 WHO classification of tumours of the central nervous system. *Acta Neuropathol* 2007; **114**: 97–109.
2. Preusser M, de Ribaupierre S, Wohrer A, Erridge SC, Hegi M, Weller M *et al.* Current concepts and management of glioblastoma. *Ann Neurol* 2011; **70**: 9–21.
3. Charles NA, Holland EC, Gilbertson R, Glass R, Kettenmann H. The brain tumor microenvironment. *Glia* 2011; **59**: 1169–1180.
4. Galli R, Binda E, Orfanelli U, Cipelletti B, Gritti A, De Vitis S *et al.* Isolation and characterization of tumorigenic, stem-like neural precursors from human glioblastoma. *Cancer Res* 2004; **64**: 7011–7021.
5. Singh SK, Hawkins C, Clarke ID, Squire JA, Bayani J, Hide T *et al.* Identification of human brain tumour initiating cells. *Nature* 2004; **432**: 396–401.
6. Venere M, Fine HA, Dirks PB, Rich JN. Cancer stem cells in gliomas: identifying and understanding the apex cell in cancer's hierarchy. *Glia* 2011; **59**: 1148–1154.
7. Chen J, Li Y, Yu TS, McKay RM, Burns DK, Kernie SG *et al.* A restricted cell population propagates glioblastoma growth after chemotherapy. *Nature* 2012; **488**: 522–526.
8. Yuki K, Natsume A, Yokoyama H, Kondo Y, Ohno M, Kato T *et al.* Induction of oligodendrogenesis in glioblastoma-initiating cells by IFN-mediated activation of STAT3 signaling. *Cancer Lett* 2009; **284**: 71–79.
9. Campos B, Wan F, Farhadi M, Ernst A, Zeppernick F, Tagscherer KE *et al.* Differentiation therapy exerts antitumor effects on stem-like glioma cells. *Clin Cancer Res* 2010; **16**: 2715–2728.
10. Piccirillo SG, Reynolds BA, Zanetti N, Lamorte G, Binda E, Broggi G *et al.* Bone morphogenetic proteins inhibit the tumorigenic potential of human brain tumour-initiating cells. *Nature* 2006; **444**: 761–765.
11. Silber J, Lim DA, Petritsch C, Persson AI, Maunakea AK, Yu M *et al.* miR-124 and miR-137 inhibit proliferation of glioblastoma multiforme cells and induce differentiation of brain tumor stem cells. *BMC Med* 2008; **6**: 14.
12. Gal H, Pandi G, Kanner AA, Ram Z, Lithwick-Yanai G, Amariglio N *et al.* MIR-451 and Imatinib mesylate inhibit tumor growth of Glioblastoma stem cells. *Biochem Biophys Res Commun* 2008; **376**: 86–90.
13. Wagenknecht B, Glaser T, Naumann U, Kugler S, Isenmann S, Bahr M *et al.* Expression and biological activity of X-linked inhibitor of apoptosis (XIAP) in human malignant glioma. *Cell Death Differ* 1999; **6**: 370–376.
14. Nagata M, Nakayama H, Tanaka T, Yoshida R, Yoshitake Y, Fukuma D *et al.* Overexpression of cIAP2 contributes to 5-FU resistance and a poor prognosis in oral squamous cell carcinoma. *Br J Cancer* 2011; **105**: 1322–1330.
15. Fulda S, Vucic D, Targeting IAP. proteins for therapeutic intervention in cancer. *Nat Rev Drug Discov* 2012; **11**: 109–124.
16. Oeckinghaus A, Hayden MS, Ghosh S. Crosstalk in NF-kappaB signaling pathways. *Nat Immunol* 2011; **12**: 695–708.
17. Varfolomeev E, Goncharov T, Fedorova AV, Dynek JN, Zobel K, Deshayes K *et al.* c-IAP1 and c-IAP2 are critical mediators of tumor necrosis factor alpha (TNFalpha)-induced NF-kappaB activation. *J Biol Chem* 2008; **283**: 24295–24299.
18. Bertrand MJ, Milutinovic S, Dickson KM, Ho WC, Boudreault A, Durkin J *et al.* cIAP1 and cIAP2 facilitate cancer cell survival by functioning as E3 ligases that promote RIP1 ubiquitination. *Mol Cell* 2008; **30**: 689–700.
19. Vallabhapurapu S, Matsuzawa A, Zhang W, Tseng PH, Keats JJ, Wang H *et al.* Nonredundant and complementary functions of TRAF2 and TRAF3 in a ubiquitination cascade that activates NIK-dependent alternative NF-kappaB signaling. *Nat Immunol* 2008; **9**: 1364–1370.
20. Zarnegar BJ, Wang Y, Mahoney DJ, Dempsey PW, Cheung HH, He J *et al.* Noncanonical NF-kappaB activation requires coordinated assembly of a regulatory complex of the adaptors cIAP1, cIAP2, TRAF2 and TRAF3 and the kinase NIK. *Nat Immunol* 2008; **9**: 1371–1378.
21. Vellanki SH, Grabrucker A, Liebau S, Proepper C, Eramo A, Braun V *et al.* Small-molecule XIAP inhibitors enhance gamma-irradiation-induced apoptosis in glioblastoma. *Neoplasia* 2009; **11**: 743–752.
22. Berger R, Jennewein C, Marschall V, Karl S, Cristofanon S, Wagner L *et al.* NF-{kappa}B is required for Smac mimetic-mediated sensitization of glioblastoma cells for {gamma}-irradiation-induced apoptosis. *Mol Cancer Ther* 2011; **10**: 1867–1875.
23. Varfolomeev E, Blankenship JW, Wayson SM, Fedorova AV, Kayagaki N, Garg P *et al.* IAP antagonists induce autoubiquitination of c-IAPs, NF-kappaB activation, and TNFalpha-dependent apoptosis. *Cell* 2007; **131**: 669–681.
24. Plenchette S, Cathelin S, Rebe C, Launay S, Ladoire S, Sordet O *et al.* Translocation of the inhibitor of apoptosis protein c-IAP1 from the nucleus to the Golgi in hematopoietic cells undergoing differentiation: a nuclear export signal-mediated event. *Blood* 2004; **104**: 2035–2043.
25. Long RM, Morrissey C, Walsh S, Hamilton HJ, Farrell N, O'Neill A *et al.* Alterations in the expression of inhibitors of apoptosis during differentiation of prostate epithelial cells. *BJU Int* 2007; **100**: 445–449.
26. Tchoghandjian A, Baeza N, Colin C, Cayre M, Metellus P, Beclin C *et al.* A2B5 cells from human glioblastoma have cancer stem cell properties. *Brain Pathol* 2010; **20**: 211–221.
27. Stock K, Kumar J, Synowitz M, Petrosino S, Imperatore R, Smith ES *et al.* Neural precursor cells induce cell death of high-grade astrocytomas through stimulation of TRPV1. *Nat Med* 2012; **18**: 1232–1238.
28. Liptay S, Schmid RM, Nabel EG, Nabel GJ. Transcriptional regulation of NF-kappa B2: evidence for kappa B-mediated positive and negative autoregulation. *Mol Cell Biol* 1994; **14**: 7695–7703.
29. Vaira S, Johnson T, Hirbe AC, Alhawagri M, Anwisye I, Sammut B *et al.* RelB is the NF-kappaB subunit downstream of NIK responsible for osteoclast differentiation. *Proc Natl Acad Sci USA* 2008; **105**: 3897–3902.
30. Muller-Sienerth N, Dietz L, Holtz P, Kapp M, Grigoleit GU, Schmuck C *et al.* SMAC mimetic BV6 induces cell death in monocytes and maturation of monocyte-derived dendritic cells. *PLoS One* 2011; **6**: e21556.

31. Abhari BA, Cristofanon S, Kappler R, von Schweinitz D, Humphreys R, Fulda S. RIP1 is required for IAP inhibitor-mediated sensitization for TRAIL-induced apoptosis via a RIP1/FADD/caspase-8 cell death complex. *Oncogene* 2013; **32**: 3263–3273.

32. Bae MK, Kim SR, Lee HJ, Wee HJ, Yoo MA, Ock OhS *et al.* Aspirin-induced blockade of NF-kappaB activity restrains up-regulation of glial fibrillary acidic protein in human astroglial cells. *Biochim Biophys Acta* 2006; **1763**: 282–289.

33. Nogueira L, Ruiz-Ontanon P, Vazquez-Barquero A, Lafarga M, Berciano MT, Aldaz B *et al.* Blockade of the NFkappaB pathway drives differentiating glioblastoma-initiating cells into senescence both in vitro and in vivo. *Oncogene* 2011; **30**: 3537–3548.

34. Sabolek M, Herborg A, Schwarz J, Storch A. Dexamethasone blocks astroglial differentiation from neural precursor cells. *Neuroreport* 2006; **17**: 1719–1723.

35. Ozeki A, Suzuki K, Suzuki M, Ozawa H, Yamashita S. Acceleration of astrocytic differentiation in neural stem cells surviving X-irradiation. *Neuroreport* 2012; **23**: 290–293.

36. De Molfetta GA, Luciola Zanette D, Alexandre Panepucci R, Dos Santos AR, da Silva Jr WA, Antonio Zago M. Role of NFKB2 on the early myeloid differentiation of CD34 + hematopoietic stem/progenitor cells. *Differentiation* 2010; **80**: 195–203.

37. Enwere EK, Holbrook J, Lejmi-Mrad R, Vineham J, Timusk K, Sivaraj B *et al.* TWEAK and cIAP1 regulate myoblast fusion through the noncanonical NF-kappaB signaling pathway. *Sci Signal* 2012; **5**: ra75.

38. Young KM, Bartlett PF, Coulson EJ. Neural progenitor number is regulated by nuclear factor-kappaB p65 and p50 subunit-dependent proliferation rather than cell survival. *J Neurosci Res* 2006; **83**: 39–49.

39. Guttridge DC, Albanese C, Reuther JY, Pestell RG, Baldwin Jr AS. NF-kappaB controls cell growth and differentiation through transcriptional regulation of cyclin D1. *Mol Cell Biol* 1999; **19**: 5785–5799.

40. Widera D, Mikenberg I, Kaltschmidt B, Kaltschmidt C. Potential role of NF-kappaB in adult neural stem cells: the underrated steersman? *Int J Dev Neurosci* 2006; **24**: 91–102.

41. Yang C, Atkinson SP, Vilella F, Lloret M, Armstrong L, Mann DA *et al.* Opposing putative roles for canonical and noncanonical NFkappaB signaling on the survival, proliferation, and differentiation potential of human embryonic stem cells. *Stem Cells* 2010; **28**: 1970–1980.

42. Liu M, Sakamaki T, Casimiro MC, Willmarth NE, Quong AA, Ju X *et al.* The canonical NF-kappaB pathway governs mammary tumorigenesis in transgenic mice and tumor stem cell expansion. *Cancer Res* 2010; **70**: 10464–10473.

43. Fulda S, Wick W, Weller M, Debatin KM. Smac agonists sensitize for Apo2L/TRAIL- or anticancer drug-induced apoptosis and induce regression of malignant glioma in vivo. *Nat Med* 2002; **8**: 808–815.

44. Wagner L, Marschall V, Karl S, Cristofanon S, Zobel K, Deshayes K *et al.* Smac mimetic sensitizes glioblastoma cells to Temozolomide-induced apoptosis in a RIP1- and NF-kappaB-dependent manner. *Oncogene* 2013; **32**: 988–997.

45. Tchoghandjian A, Jennewein C, Eckhardt I, Rajalingam K, Fulda S. Identification of non-canonical NF-kappaB signaling as a critical mediator of Smac mimetic-stimulated migration and invasion of glioblastoma cells. *Cell Death Dis* 2013; **4**: e564.

46. Vogler M, Durr K, Jovanovic M, Debatin KM, Fulda S. Regulation of TRAIL-induced apoptosis by XIAP in pancreatic carcinoma cells. *Oncogene* 2007; **26**: 248–257.

47. Kasperczyk H, La Ferla-Bruhl K, Westhoff MA, Behrend L, Zwacka RM, Debatin K-M *et al.* Betulinic acid as new activator of NF-kappaB: molecular mechanisms and implications for cancer therapy. *Oncogene* 2005; **24**: 6945–6956.

48. Takizawa T, Nakashima K, Namihira M, Ochiai W, Uemura A, Yanagisawa M *et al.* DNA methylation is a critical cell-intrinsic determinant of astrocyte differentiation in the fetal brain. *Dev Cell* 2001; **1**: 749–758.

49. Karl S, Pritschow Y, Volcic M, Hacker S, Baumann B, Wiesmuller L *et al.* Identification of a novel pro-apoptotic function of NF-kappaB in the DNA damage response. *J Cell Mol Med* 2009; **13**: 4239–4256.

Supplementary Information accompanies this paper on Cell Death and Differentiation website (http://www.nature.com/cdd)